Supplementary Material (ESI) for Chemical Science
This journal is © The Royal Society of Chemistry 2011

Electronic Supplementary Information

Conformational Analysis of Supramolecular Polymerization Processes of Disc-like Molecules

Yoko Nakano, Takashi Hirose, Patrick J. M. Stals, E. W. Meijer*, Anja R. A. Palmans*

Laboratory of Macromolecular and Organic Chemistry and Institute for Complex Molecular Systems, Eindhoven University of Technology, P.O. Box 513, 5600 MB Eindhoven, The Netherlands

*To whom correspondence should be addressed. Email: e.w.meijer@tue.nl; a.palmans@tue.nl

Contents

Supplementary Material (ESI) for Chemical Science
This journal is © The Royal Society of Chemistry 2011

Experimental section

Materials & Methods

The solvent, *n*-heptane, *iso*-octane, and MCH were obtained in spectrophotometric grade from Acros, Merck, and Aldrich respectively, and used as received. Decahydronaphthalene was obtained as a mixture of *cis*- and *trans*- isomers for synthesis grade from Merck and used as received. All other chemicals were obtained from either Acros or Aldrich and used as received. Asymmetrically substituted BTAs (**1a**–**c**) were synthesised and characterized in accordance with published procedures.[1] ^{1}H-NMR measurements were conducted on a Varian Mercury 200 MHz and/or a Varian Gemini 400 MHz. Proton chemical shifts are reported in ppm downfield from tetramethylsilane (TMS). Maldi-TOF-MS were acquired using a Perserptive Biosystem Voyager-DE PRO spectrometer, α-cyano-4-hydroxycinnamic acid was employed as the matrix material. IR spectra were recorded on a Perkin Elmer spectrum 1 using a universal ATR. The thermal transitions were determined with DSC using a TA Q2000 DSC under a nitrogen atmosphere with heating and cooling rates of 10 K/min. CD and UV measurements were performed on a Jasco J-815 spectropolarimeter where the sensitivity, time constant and scan rate were chosen appropriately. All measurements were done in a 10 mm quartz cell. Corresponding temperature-dependent measurements were performed with a PFD-425S/15 Peltier-type temperature controller with a temperature range from −10 °C to 110 °C and adjustable temperature slope. In all experiments, the linear dichroism was also measured and in all cases no linear dichroism was observed. The solution infrared spectra were recorded with a Perkin-Elmer spectrum 1 and measured at a resolution of 4 cm^{-1}, by coadding 128 scans. Samples were held in a fixed path length (50 μm) cell with CaF_2 windows.

Theoretical calculations

Regarding the long computational time necessary to fully optimize the geometry of self-assembled stacking of BTAs within density functional theory (DFT) calculations, and further to determine the frequencies, the dipolar and rotational strength, it was necessary to simplify the system prior to the calculations. To this end, the three aliphatic side chains were replaced by methyl groups in a monomer system.

Supplementary Material (ESI) for Chemical Science
This journal is © The Royal Society of Chemistry 2011

The geometry optimizations, vibrational frequencies, and time-dependent transition states were calculated by Gaussian 03 program.[2] Calculation of the optimized geometries of a monomer was performed at the DFT level using B3LYP functional and 6-31G(d) basis set. Successive TD calculation was performed at the level of PBE1PBE/6-31++G(2d,p) level.[3] The line spectra of TD-DFT calculations were convoluted using Gaussian curves to create theoretical UV-vis and circular dichroism spectra. The convoluted spectra were generated by GaussSum application (version 2.2)[4] with the parameters of FWHM = 3000 cm^{-1} for UV-vis and sigma = 0.5 eV for CD spectra, respectively.

MacroModel Calculations

Molecular mechanics calculations were carried out by MacroModel program, Maestro version 9.0.211. Geometrical optimization were performed with PRCG method using OPLS_2005 force field in a gas phase (dielectric constant = 1.0). An achiral 8-mers structure forming [*P*]-helix geometry was initially generated and energetically minimized. Chiral four 8-mer structures, that is the structures having stereogenic methyl groups at the α- and β-position of side chains with (*R*)- and (*S*)-configuration, were constructed based on the optimized achiral structure. The optimized potential energies of α-(*R*), α-(*S*), β-(*R*), and β-(*S*) structures were −1742.026 kJ/mol, −1603.356 kJ/mol, −1993.324 kJ/mol, and −2026.825 kJ/mol, respectively. The potential energy values of [*P*]-helix geometry of 8-mers imply an odd–even effect; the α-(*R*) structure (i.e. the structure of (*R*)-configuration at α-position) is more stable than α-(*S*) structure, whereas the β-(*S*) structure is more stable than β-(*R*). In other words, α-(*S*)-substituted 8-mers prefers the [*M*]-helix geometry and β-(*S*)-substituted 8-mers prefers the [*P*]-helix geometry, since reflection of geometry keeps energy. In Figure 6 in the main text, the [*M*]-helix geometry of the α-(*S*)-substituted structure (left, red) and the [*P*]-helix geometry of the β-(*S*)-substituted structure (right, blue) are shown. The former [*M*]-helix geometry of (*S*)-substituted structure was generated by the reflection of the [*P*]-helix geometry of the α-(*R*) structure.

Synthesis and characterization of BTA (1d):

Supplementary Material (ESI) for Chemical Science
This journal is © The Royal Society of Chemistry 2011

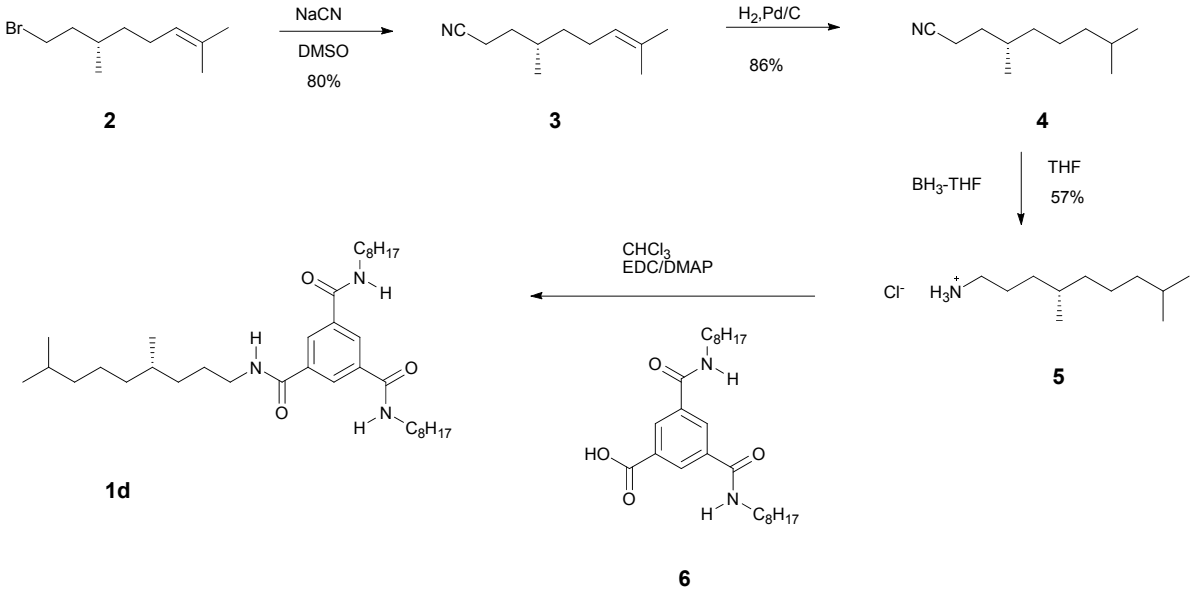

Scheme S1 Synthesis of **1d**

*Synthesis of (S)-4,8-dimethylnon-7-enenitrile (**3**)*

A 250 mL three-necked round-bottom flask was charged with a solution of *(S)*-8 bromo-2,6-dimethyloct-2-ene (4.88 g, 0.022 mol) in DMSO (50 mL) under an argon atmosphere with a gas wash bottle filled with aqueous NaOH (1 M) at the end of the gasflow. The mixture was heated to 50 °C. Subsequently, 1.1 equivalents NaCN (1.22 g, 0.025 mol) was added to the solution and the mixture was stirred overnight at 50 °C under an argon atmosphere. After the reaction was completed, the mixture was allowed to cool down to room temperature, after which it was transferred to a separation funnel and water (400 mL) was added. The water layer was extracted with CH_2Cl_2 (3 × 75 mL), the organic layers were collected and washed with aqueous KCl (1 M, 3 × 50 mL). After evaporation *in vacuo* the crude product was obtained as a yellowish oil, which was used without further purification. (2.89 g, 80%). ^{1}H-NMR ($CDCl_3$): δ_H = 5.09 (1 H, t, *H*-C=C), 2.35 (2 H, t, NC-C*H*$_2$), 2.17–1.88 (2 H, m, C=C-C*H*$_2$), 1.78–1.12 (11 H, m, C*H*$_2$, C*H*, C=C-C*H*$_3$), 0.93 (3 H, d, *J* = 6.6 Hz, CH-C*H*$_3$).

*Synthesis of (S)-4,8-dimethylnonanenitrile (**4**)*

A 250 mL reactor was charged with a solution of *(S)*-4,8-dimethylnon-7-enenitrile (2.8 g, 0.017 mol) in MeOH (50 mL) and subsequently flushed with argon for 2 hours, whereafter Pd/C was added. The reaction mixture was shaken for 3 hours under a pressure of 60 psi of hydrogen, filtered and the solvent was removed *in vacuo* to yield the pure product as

Supplementary Material (ESI) for Chemical Science
This journal is © The Royal Society of Chemistry 2011

a yellowish oil, which was used without further purification (2.52 g, 89%). ^{1}H-NMR ($CDCl_3$): δ_H = 2.35 (2 H, t, CN-C*H*$_2$), 1.78–1.12 (10 H, m, C*H*, C*H*$_2$), 0.93–0.82 (9 H, m, C*H*$_3$).

*Synthesis of (S)-4,8-dimethylnonan-1-amine·HCl (**5**)*

A 250 mL three-necked round-bottom flask was charged with a solution of borane-THF-complex (1 M, 30 mL), while cooling to 0 °C and keeping the solution under an argon atmosphere. To this solution a solution containing *(S)*-4,8-dimethylnonanenitrile (2.52 g, 0.015 mol) in dry THF (12.5 mL) was slowly added via a dropping funnel. The mixture was stirred for 30 minutes at 0 °C, after which the mixture was refluxed for 1 hour. Finally the mixture was stirred overnight at room temperature. After this, the mixture was cooled to 0 °C, and methanol (30 mL) was slowly added dropwise. Hydrochloric acid (37% in water, 3.5 mL) was added slowly; the reaction mixture was stirred for 1 hour and subsequently evaporated to dryness *in vacuo*. To the resulting viscous liquid was added aqueous NaOH (2 M, 50 mL) and this solution was extracted with diethyl ether (3 × 100 mL). The organic layers were collected and dried with sodium sulfate, filtered and the solvent was removed *in vacuo* to obtain a yellowish liquid. The crude product was than dissolved in methyl *t*-butylether (15 mL) and to this solution was added aqueous HCl (5 N) in 2-propanol (2 mL), the resulting suspension was filtered and the solid residue was dried to yield the title compound as an off-white solid (1.78 g, 57%). ^{1}H-NMR ($CDCl_3$): δ_H = 8.29 (3 H, br s, N*H*$_3$), 2.96 (2 H, t, NH_3^+-C*H*$_2$), 2.06–1.61 (2 H, m, NH_3^+-CH_2-C*H*$_2$), 1.63–1.02 (10 H, m, C*H*, C*H*$_2$), 0.89–0.82 (9 H, m, C*H*$_3$).

*Synthesis of (S)-N′-(4,8-dimethylnonyl)-N″,N‴-di-n-octylbenzene-1,3,5-tricarboxamide (**1d**)*

(S)-N′-(4,8-dimethylnonyl)-*N″*,*N‴*-di-*n*-octylbenzene-1,3,5-tricarboxamide (**1d**) was synthesised following a procedure described previously.[1] **1d** was obtained as a sticky white solid (0.136 g, 66%). ^{1}H-NMR ($CDCl_3$): δ_H = 8.34 (3 H, s, Ar-*H*), 6.46 (3 H, t, N-*H*), 3.45 (6 H, m, NH-C*H*$_2$), 1.71–1.02 (36 H, m, C*H*, C*H*$_2$), 0.92–0.84 (15 H, m, C*H*$_3$); IR: ν_{max}/cm^{-1} 3309 (N-H stretch), 1641 (C=O), 1530 (amide II); MS (Maldi-TOF): *m*/*z*: 608.44 $[M + Na]^+$; observed DSC transitions: $T_{Colho->iso}$= 212.8 ºC, ΔH= 18 kJ mol^{-1}.

CD spectra

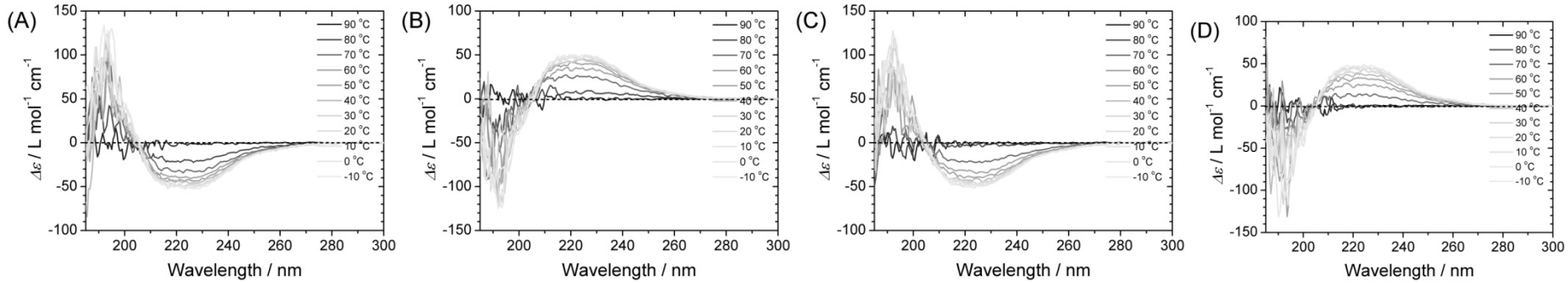

UV spectra

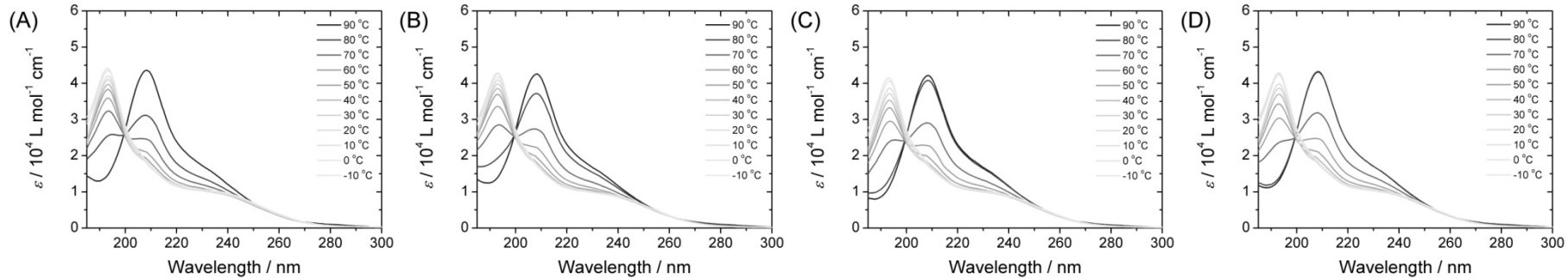

Figure S1 CD (top) and UV (bottom) spectra of **1a** (A), **1b** (B), **1c** (C), **1d** (D) in *n*-heptane (30 μM) at temperature between 90 °C and −10 °C with a cooling rate of 1 °C min^{-1}.

CD spectra

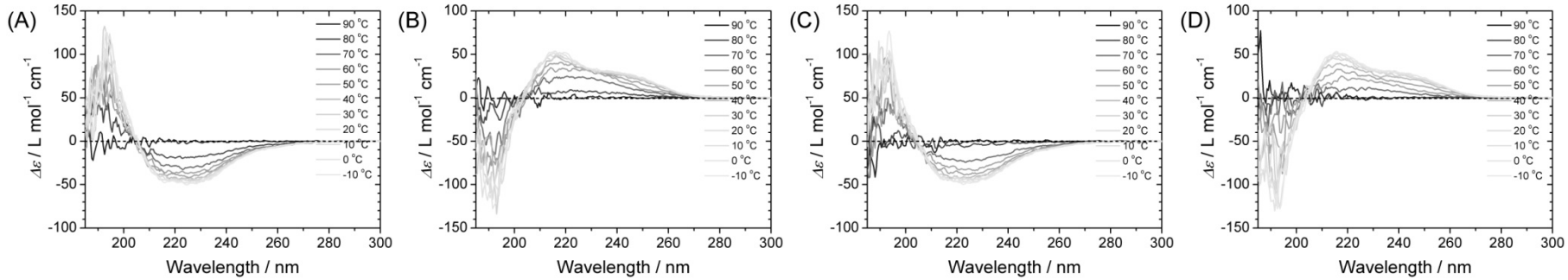

UV spectra

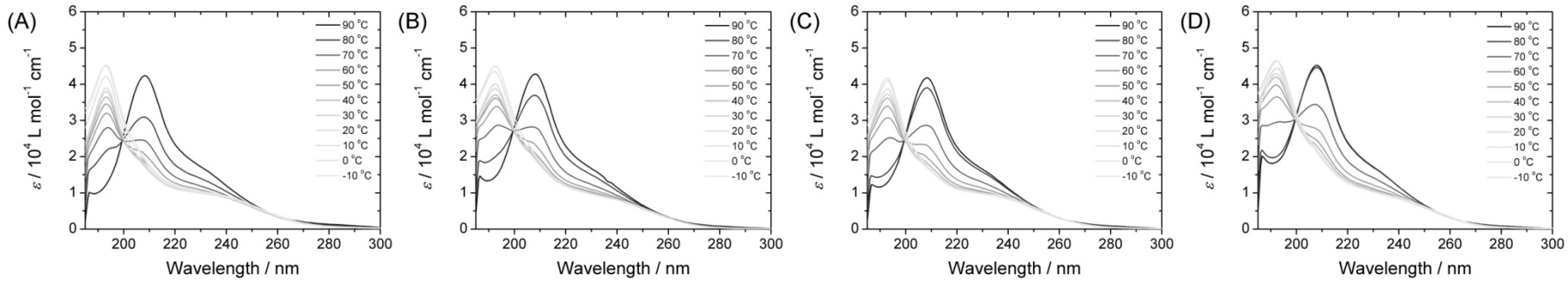

Figure S2 CD (top) and UV (bottom) spectra of **1a** (A), **1b** (B), **1c** (C), **1d** (D) in *iso*-octane (30 μM) at temperature between 90 °C and −10 °C with a cooling rate of 1 °C min^{-1}.

CD spectra

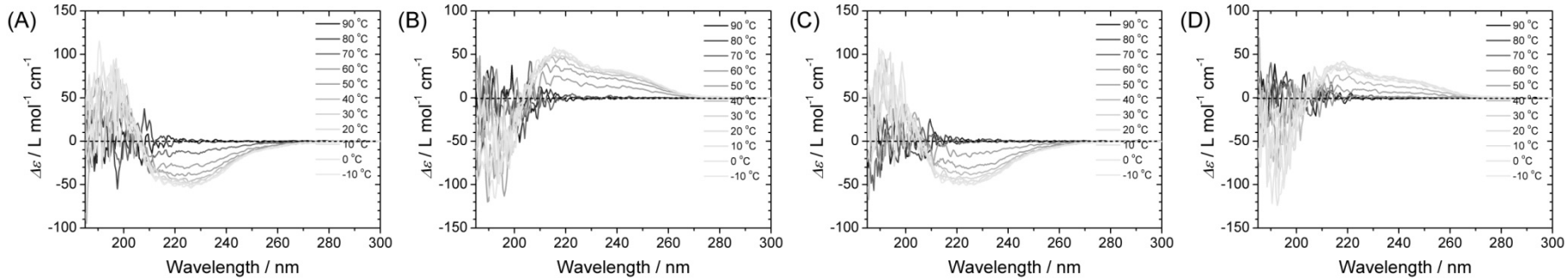

UV spectra

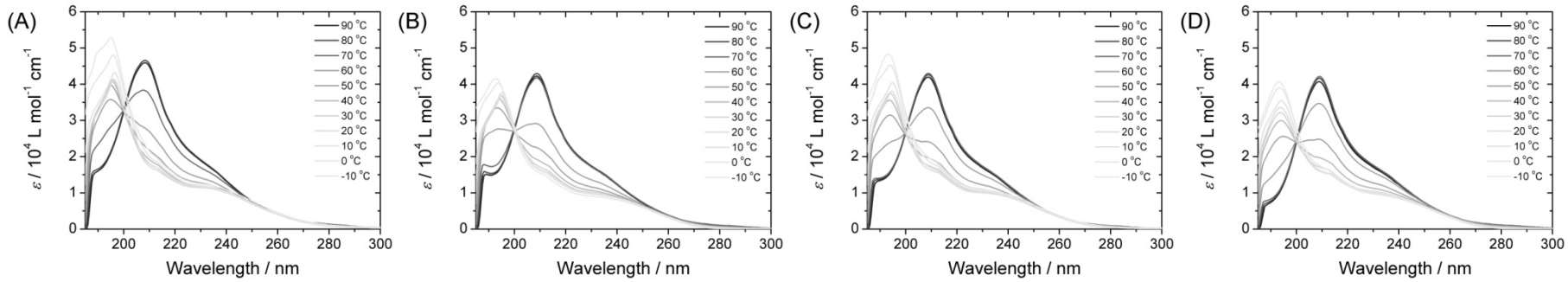

Figure S3 CD (top) and UV (bottom) spectra of **1a** (A), **1b** (B), **1c** (C), **1d** (D) in MCH (30 μM) at temperature between 90 °C and −10 °C with a cooling rate of 1 °C min^{-1}.

CD spectra

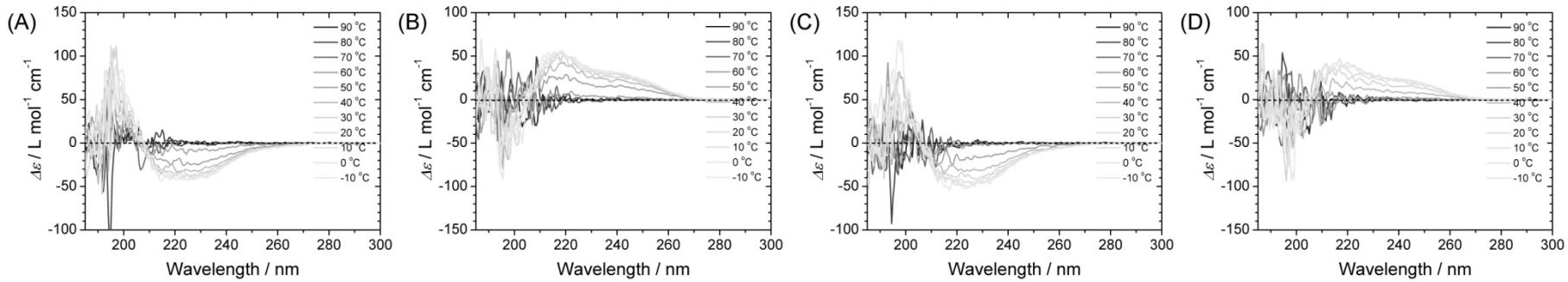

UV spectra

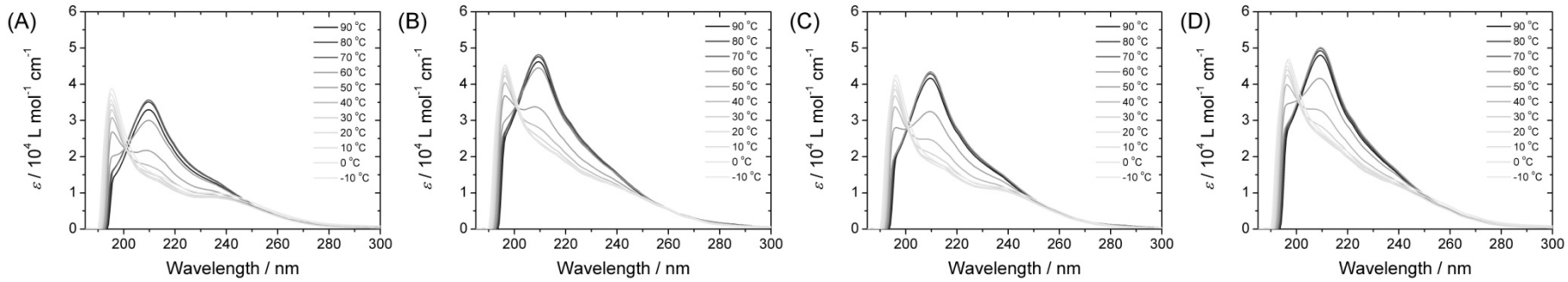

Figure S4 CD (top) and UV (bottom) spectra of **1a** (A), **1b** (B), **1c** (C), **1d** (D) in DHN (30 μM) at temperature between 90 °C and −10 °C with a cooling rate of 1 °C min^{-1}.

Supplementary Material (ESI) for Chemical Science
This journal is © The Royal Society of Chemistry 2011

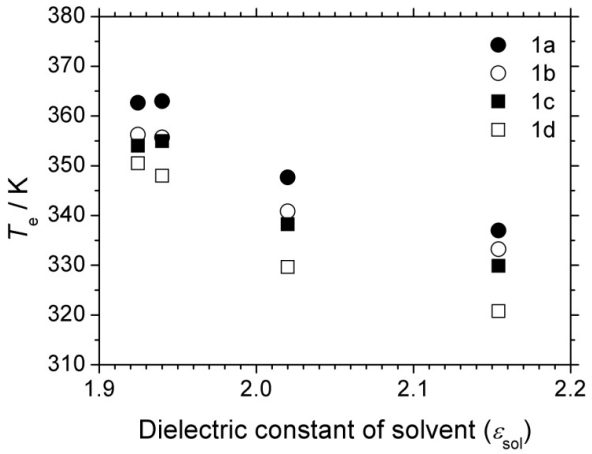

Figure S5 The T_e values of **1a–d** as a function of the dielectric constants of solvent, ε_{sol}.

Supplementary Material (ESI) for Chemical Science
This journal is © The Royal Society of Chemistry 2011

Table S1 Molecular areas and volumes computed by Winmostar [a]

Compounds	van der Waals [b]					Accessible surface [c]				
	Area / Å^2	Volume / Å^3	Ovality [d]	Max length / Å	Max radius / Å	Area / Å^2	Volume / Å^3	Ovality [d]	Max length / Å	Max radius / Å
n-heptane	180.163	129.493	1.45551	11.886	5.950	427.320	719.560	1.10042	15.886	7.950
iso-octane	195.347	145.979	1.45701	9.269	4.793	415.420	728.847	1.06067	13.269	6.793
MCH	156.068	118.118	1.34003	8.445	4.372	373.334	628.725	1.05190	12.445	6.372
DHN	197.934	157.477	1.40353	9.728	4.864	428.450	762.120	1.06186	13.728	6.864

[a] Every structure was optimized by Gaussian with B3LYP/6-31g(d) level
[b] The van der Waals (vdw) surface is generated by substituting every atoms with spheres having van der Waals radius.
[c] The accessible surface is the locus of the center of a small solvent sphere (2.0 Å radius) tracing the vdw surface.
[d] Ovality is defined as molecular surface area divided by minimum surface area, where minimum surface area is the surface area of a (complete) sphere having the identical volume.

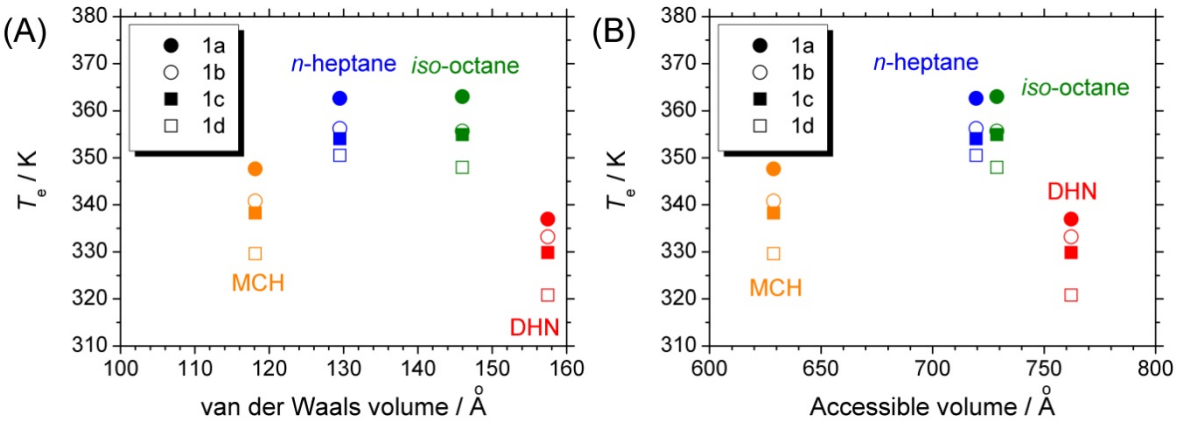

Figure S6 The T_e values of **1a–d** as a function of van der Waals volume (A) and accessible volume (B) of the solvent molecules calculated by Winmostar.

Supplementary Material (ESI) for Chemical Science
This journal is © The Royal Society of Chemistry 2011

Table S2 Molecular aspect ratio computed by Winmostar [a]

Compounds	Number of atoms	Molecular weight	Length of x-axis (L) [b] / Å	Length of y-axis (D) [c] / Å	Aspect ratio (L/D) [d]
n-heptane	23	100.20	11.886	5.189	2.29
iso-octane	26	114.23	9.184	6.741	1.36
MCH	21	98.19	8.386	6.751	1.24
DHN	28	138.25	9.286	7.408	1.25

[a] Every structure was optimized by Gaussian with B3LYP/6-31g(d) level
[b] Length of the cylinder having minimum diameter in which the molecule inscribes
[c] Diameter of the cylinder having minimum diameter in which the molecule inscribes
[d] Aspect ratio is defined by the length divided by the diameter of the cylinder

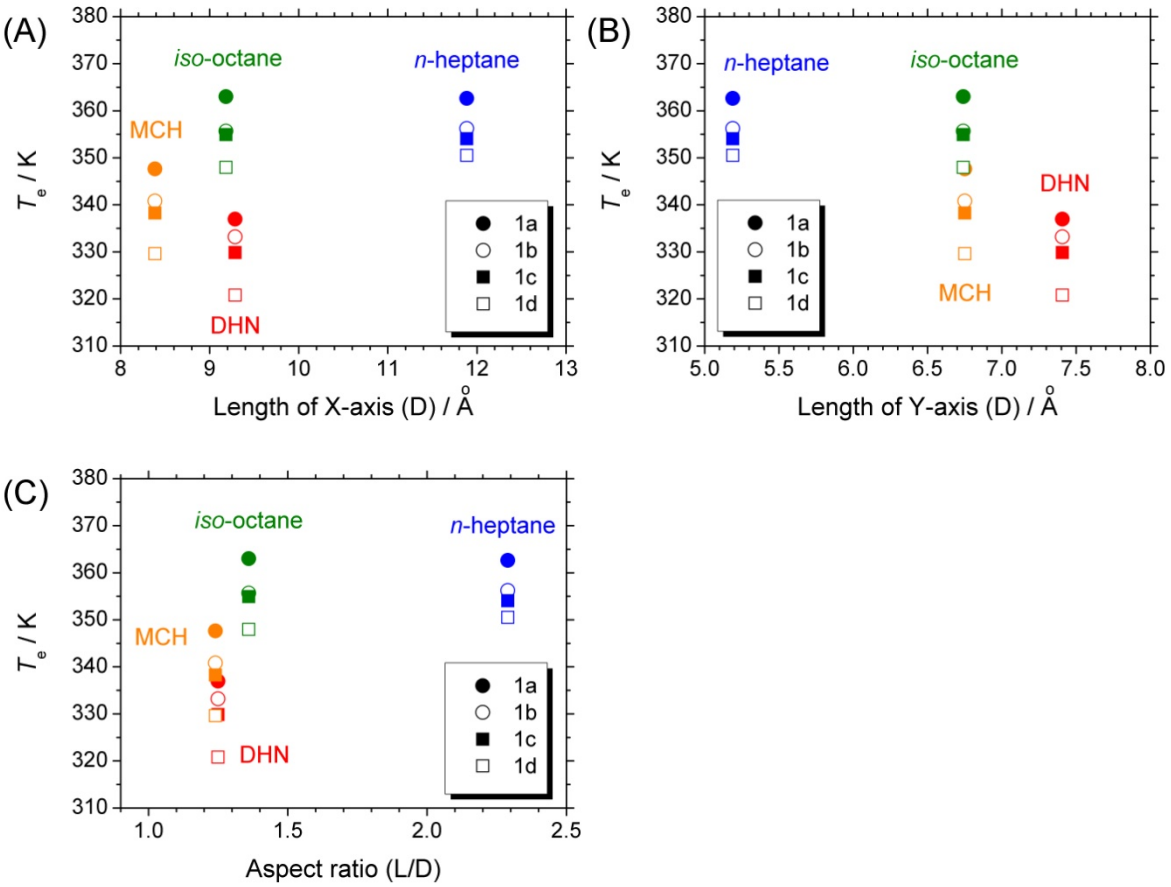

Figure S7 The T_e values of **1a–d** as a function of length of x-axis (A), y-axis (B) and aspect ratio (C) of the solvent molecules calculated by Winmostar.

Supplementary Material (ESI) for Chemical Science
This journal is © The Royal Society of Chemistry 2011

Table S3 Molecular surface computed by MacroModel [a]

Compounds	Van der waals Surface Area	Surface (probe radius = 1.4 Å) Surface Area
n-heptane	177.588	162.971
iso-octane	192.686	164.235
MCH	153.901	139.038
DHN	195.313	172.055

[a] Every structure was optimized by Gaussian with B3LYP/6-31g(d) level

Table S4 Molecular surface computed by Gaussian (B3LYP/6-31g(d) with keyword of 'volume = tight') [a]

Compounds	Molar volume bohr^3/mol	Molar volume cm^3/mol	a0 for SCRF Å	a0 for SCRF bohr
n-heptane	1220.586	108.924	4.36	8.24
iso-octane	1476.142	131.729	4.61	8.72
MCH	1119.982	99.946	4.25	8.04
DHN	1458.936	130.194	4.60	8.69

[a] Every structure was optimized by Gaussian with B3LYP/6-31g(d) level

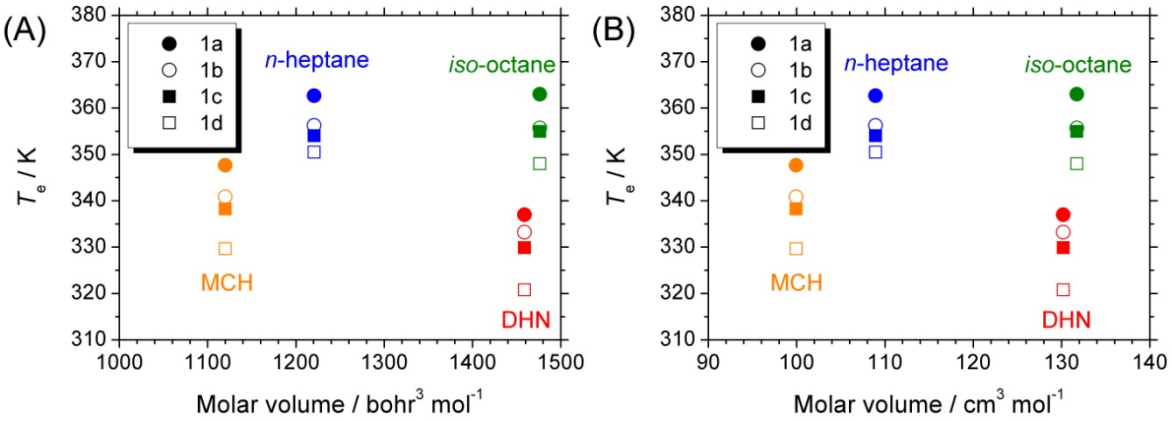

Figure S8 The T_e values of **1a–d** as a function of molar volume in bohr^3 mol^{-1} (A), in cm^3 mol^{-1} (B) of the solvent molecules calculated by Gaussian.

Supplementary Material (ESI) for Chemical Science
This journal is © The Royal Society of Chemistry 2011

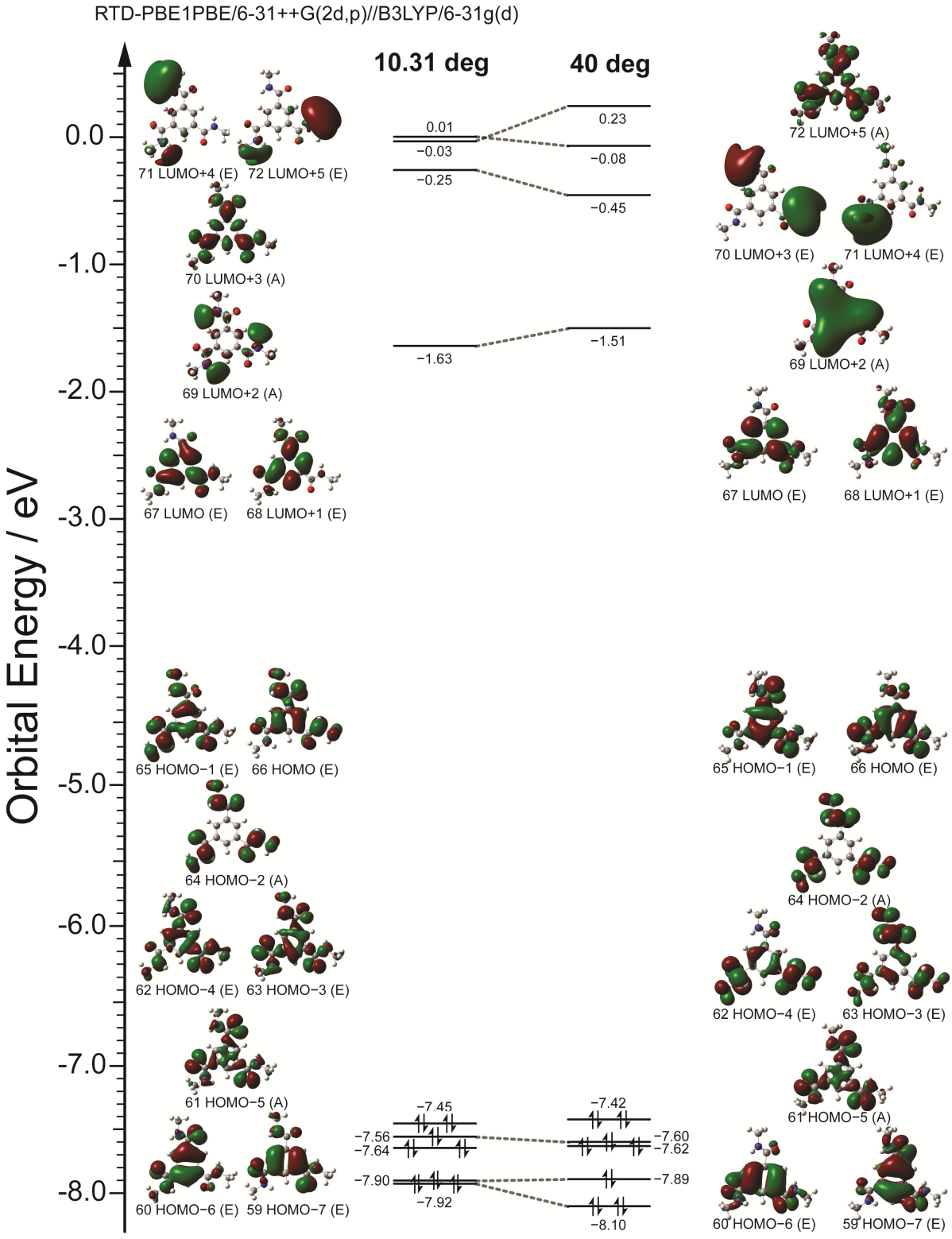

Figure S9 The orbital correlation diagram of **1e** calculated with a RTD-PBE1PBE/6-31++G(2d,p)//B3LYP/6-31G(d) level.

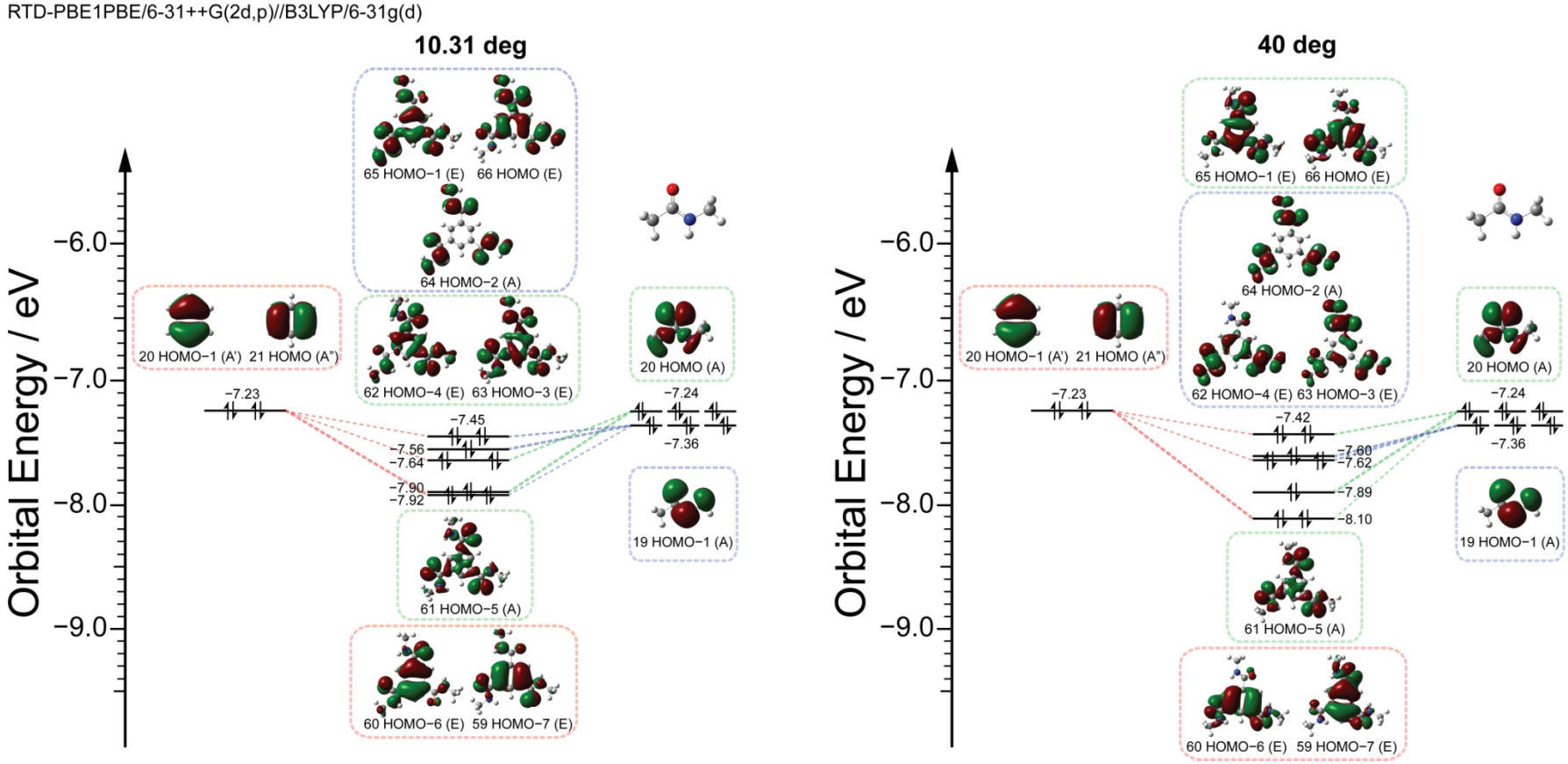

Figure S10 The comparison of the electron orbitals of **1e** to that of benzene and *N*-methylacetamide around the HOMO region.

Free optimized (C=O dihedral angle = 10.311°)

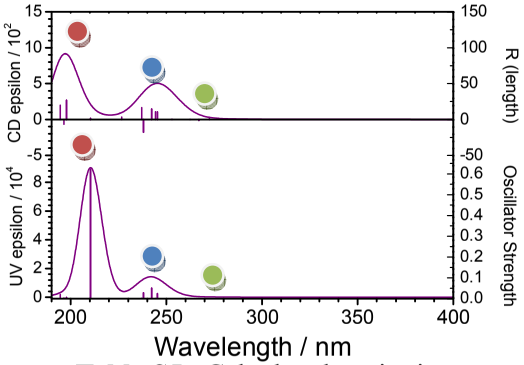

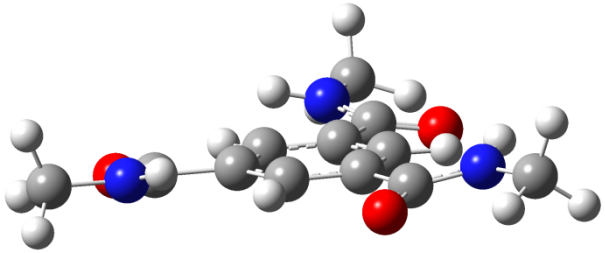

Table S5 Calculated excitation states of BTA with C=O dihedral angle of 10.311° by TD-DFT (PBE1PBE/6-31++g(2d,p)//B3LYP/6-31g(d) level)

States	Main configurations (|C| > 0.2) (~configuration > 8%)	Direction of Transition	Excitation Energy in eV (nm)	Oscillator Strength Osc. (UV)	Oscillator Strength R_{length} (CD)
1	0.30 (65→67) + 0.30 (66→68) + 0.27 (62→67) – 0.27 (63→68) +0.21 (62→68) + 0.21 (63→67)	Z	4.56 (272)	0.0002	2.683
2	0.32 (**62→67**) + 0.32 (**63→68**) + 0.31 (**61→67**)	**XY**	4.65 (267)	0.0010	−1.1656
3	0.32 (**63→67**) – 0.32 (**62→68**) + 0.31 (**61→68**)	**YX**	4.65 (267)	0.0010	−1.1700
4	0.31 (62→68) + 0.31 (63→67) – 0.28 (59→68) – 0.28 (60→67) – 0.22 (65→67) – 0.22 (66→68)	Z	4.74 (262)	0.0000	0.0595
5	0.41 (65→68) – 0.41 (66→67) + 0.20 (65→67) + 0.20 (66→68)	Z	4.91 (252)	0.0000	0.2591
6	0.49 (**64→67**) + 0.27 (**65→68**) + 0.27 (**66→67**)	**X**	5.06 (245)	**0.0228**	**10.4977**
7	0.49 (**64→68**) + 0.27 (**65→67**) − 0.27 (**66→68**)	**Y**	5.06 (245)	**0.0228**	**10.4720**
8	0.31 (63→68) − 0.31 (62→67) + 0.29 (62→68) + 0.29 (63→67)	Z	5.08 (244)	0.0009	**10.4774**
9	0.26 (**64→68**) – 0.26 (**65→67**) + 0.26 (**66→68**) + 0.25 (**64→67**)	**Y**	5.13 (242)	**0.0486**	**14.0215**
10	0.26 (**64→67**) – 0.26 (**65→68**) − 0.26 (**66→67**) − 0.25 (**64→68**)	**X**	5.13 (242)	**0.0486**	**14.0057**
11	0.49 (**61→68**) + 0.30 (**64→68**)	**XY**	5.22 (238)	**0.0296**	**−17.6243**
12	0.49 (**61→67**) + 0.30 (**64→67**)	**XY**	5.22 (238)	**0.0296**	**−17.6206**
13	0.34 (59→68) + 0.34 (60→67) − 0.25 (65→67) − 0.25 (66→68)	Z	5.24 (237)	0.0018	**17.2343**
14	0.43 (60→68) − 0.43 (59→67)	Z	5.49 (226)	0.0003	3.4422
15	0.39 (**59→68**) − 0.39 (**60→67**)	**Y**	5.91 (210)	**0.6255**	1.7479
16	− 0.39 (**59→67**) − 0.39 (**60→67**)	**X**	5.91 (210)	**0.6254**	1.1550
17	0.51 (**66→69**) + 0.24 (**64→71**)	**YX**	6.24 (199)	0.0033	**19.7697**
18	0.51 (**65→69**) − 0.24 (**64→72**)	**XY**	6.24 (199)	0.0033	**19.7629**
19	0.51 (64→69) − 0.21 (65→72) + 0.21 (66→71) + 0.21 (65→71) + 0.21 (66→72)	Z	6.28 (197)	0.0026	−6.1196
20	0.40 (**63→70**) – 0.37 (**66→70**) + 0.24 (**63→69**)	**Y**	6.38 (194)	0.0191	**20.1653**

C=O dihedral angle fixed to 40°

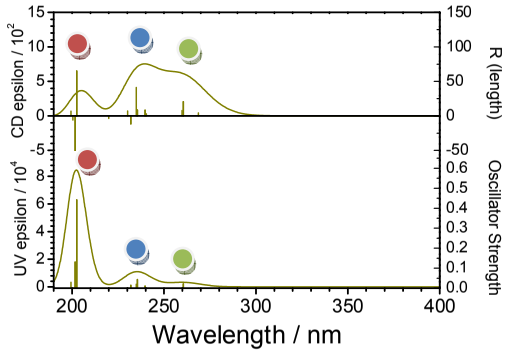

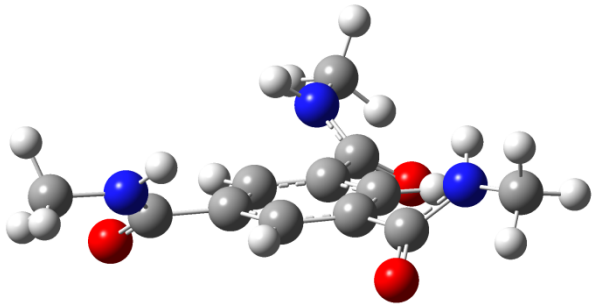

Table S6 Calculated excitation states of BTA with C=O dihedral angle of 40° by TD-DFT (PBE1PBE/6-31++g(2d,p)//B3LYP/6-31g(d) level)

States	Main configurations (|C| > 0.2) (~configuration > 8%)	Direction of Transition	Excitation Energy in eV (nm)	Oscillator Strength Osc. (UV)	Oscillator Strength R_{length} (CD)
1	0.38 (65→68) + 0.38 (66→67) + 0.26 (65→67) – 0.26 (66→68)	Z	4.61 (269)	0.0002	4.3417
2	0.33 (**65→68**) − 0.33 (**66→67**) + 0.23 (**61→68**)	**YX**	4.76 (261)	**0.0216**	**20.5570**
3	− 0.33 (**65→67**) – 0.33 (**66→68**) + 0.23 (**61→67**)	**XY**	4.76 (261)	**0.0216**	**20.5422**
4	− 0.38 (65→67) + 0.38 (66→68) + 0.24 (65→68) + 0.24 (66→67)	Z	4.77 (260)	0.0004	**7.6748**
5	0.41 (62→68) + 0.41 (63→67)	Z	5.16 (240)	0.0012	3.0609
6	0.52 (**64→67**) − 0.25 (**61→67**)	**YX**	5.17 (240)	0.0107	**8.2351**
7	0.52 (**64→68**) − 0.25 (**61→68**)	**XY**	5.17 (240)	0.0107	**8.2293**
8	− 0.36 (**62→68**) + 0.36 (**63→67**) + 0.31 (**64→68**) + 0.23 (**61→68**)	**YX**	5.26 (236)	**0.0434**	**8.5871**
9	0.36 (**62→67**) + 0.36 (**63→68**) + 0.31 (**64→67**) + 0.23 (**61→67**)	**XY**	5.26 (236)	**0.0434**	**8.5833**
10	0.47 (**62→67**) – 0.47 (**63→68**)	Z	5.28 (235)	**0.0195**	**41.1492**
11	0.49 (**61→67**) + 0.26 (**64→67**) – 0.25 (**62→67**) – 0.25 (**63→68**)	**YX**	5.35 (232)	**0.0140**	**−11.7277**
12	0.49 (**61→68**) + 0.26 (**64→68**) + 0.25 (**62→68**) – 0.25 (**63→67**)	**XY**	5.35 (232)	**0.0140**	**−11.7306**
13	− 0.43 (59→67) + 0.43 (60→68) − 0.23 (62→68) − 0.23 (63→67)	Z	5.39 (230)	0.0023	6.9822
14	0.45 (59→68) + 0.45 (60→67)	Z	5.64 (220)	0.0007	−3.6001
15	0.28 (**59→68**) − 0.28 (**60→67**) + 0.25 (**66→69**) + 0.21 (**59→67**) +0.21 (**60→68**)	**YX**	6.12 (202)	**0.4411**	**65.3542**
16	0.28 (**59→67**) + 0.28 (**60→68**) + 0.25 (**65→69**) − 0.21 (**59→68**) +0.21 (**60→67**)	**XY**	6.12 (202)	**0.4414**	**64.5094**
17	0.50 (**66→69**) + 0.29 (**63→69**)	**Y**	6.15 (202)	**0.1312**	**−52.6780**
18	0.50 (**65→69**) + 0.24 (**62→69**)	**X**	6.15 (202)	**0.1303**	**−52.3757**
19	0.58 (64→69) − 0.21 (62→71) − 0.21 (63→70)	Z	6.19 (200)	0.0006	−6.2133
20	0.42 (**62→69**) + 0.28 (**63→69**) − 0.27 (**66→69**) – 0.21 (**65→69**)	**XY**	6.22 (199)	0.0295	6.7402

Table S7 Main configurations of the transition state 2 or 3

C=O dihedral angle	Main configurations (|C| > 0.2) (~ > 8%) and configurations from the π–π* transition (|C| > 0.1)	States	Excitation Energy in eV (nm)	Oscillator Strength Osc. (UV)	Oscillator Strength R_{length} (CD)
10°	Main: 0.32 (**62→67**) + 0.32 (**63→68**) + 0.31 (**61→67**) π–π*: n/a	**2**	4.65 (267)	0.0010	−1.1656
20°	Main: 0.30 (**65→68**) + 0.30 (**66→67**) + 0.28 (**61→67**) + 0.23 (**62→67**) + 0.23 (**63→68**) π–π*:− 0.15 (59→67) + 0.15 (60→68)	**2**	4.65 (266)	0.0054	3.0106
30°	Main: 0.36 (**65→68**) + 0.36 (**66→67**) − 0.25 (**61→68**) π–π*:− 0.16 (59→68) + 0.16 (60→67)	**2**	4.69 (264)	0.0130	10.8573
35°	Main: − 0.34 (**65→68**) − 0.34 (**66→67**) − 0.26 (**61→68**) π–π*: 0.15 (59→68) − 0.15 (60→67)	**2**	4.72 (263)	0.0169	**15.2258**
40°	Main: 0.33 (**65→68**) − 0.33 (**66→67**) + 0.23 (**61→68**) π–π*: 0.15 (59→68) − 0.15 (60→67)	**2**	4.76 (261)	**0.0216**	**20.5570**
45°	Main: 0.37 (**65→68**) + 0.37 (**66→67**) + 0.26 (**61→68**) π–π*: 0.16 (59→68) − 0.16 (60→67)	**3**	4.81 (258)	**0.0267**	**26.0022**
50°	Main: − 0.39 (**65→68**) + 0.39 (**66→67**) + 0.25 (**61→68**) π–π*: − 0.12 (59→68) + 0.12 (60→67) − 0.11 (59→67) − 0.11 (60→68)	**3**	4.87 (255)	**0.0317**	**31.2810**
60°	Main: − 0.31 (**65→68**) + 0.31 (**66→67**) + 0.24 (**65→67**) + 0.24 (**66→68**)+ 0.21 (**61→68**) π–π*: − 0.16 (59→67) + 0.16 (60→68)	**3**	5.00 (248)	**0.0394**	**40.2162**
70°	Main: 0.38 (**65→68**) + 0.38 (**66→67**) π–π*: 0.16 (59→68) − 0.13 (60→67)	**3**	5.17 (240)	**0.0479**	**45.9943**
80°	Main: 0.37 (**65→68**) + 0.37 (**66→67**) π–π*: 0.16 (59→68) + 0.16 (60→67)	**3**	5.36 (231)	**0.0584**	**43.5310**
90°	Main: 0.31 (**65→68**) + 0.31 (**66→67**) π–π*: − 0.13 (59→67) − 0.13 (60→68) + 0.13 (59→68) − 0.13 (60→67)	**3**	5.48 (226)	0.0811	−11.6918

Table S8 The orbital energies of molecular orbitals from MO59 (HOMO−7) to MO66 (HOMO) depending on the C=O dihedral angle (in eV)

	C=O dihedral angles **10°**	20°	30°	35°	**40°**	45°	50°	60°	70°	80°	90°
MO67, 68	**−1.63 (E)**	−1.61 (E)	−1.56 (E)	−1.56 (E)	−1.51 (E)	−1.42 (E)	−1.37 (E)	−1.23 (E)	−1.08 (E)	−0.93 (E)	−0.87 (E)
MO65, 66	**−7.45 (E)**	−7.43 (E)	−7.41 (E)	−7.43 (E)	**−7.42 (E)**	−7.38 (E)	−7.36 (E)	−7.33 (E)	−7.31 (E)	−7.28 (E)	−7.25 (E)
MO64	**−7.56 (A)**	−7.55 (A)	−7.56 (A)	−7.59 (A)	**−7.60 (A)**	−7.58 (A)	−7.59 (A)	−7.61 (A)	−7.63 (A)	−7.64 (E)	−7.63 (E)
MO63	**−7.64 (E)**	−7.62 (E)	−7.60 (E)	−7.63 (E)	**−7.62 (E)**	−7.59 (E)	−7.60 (E)	−7.62 (E)	−7.63 (E)	−7.64 (E)	−7.63 (E)
MO62	**−7.64 (E)**	−7.62 (E)	−7.60 (E)	−7.63 (E)	**−7.62 (E)**	−7.59 (E)	−7.60 (E)	−7.62 (E)	−7.63 (E)	−7.64 (A)	−7.64 (A)
MO61	**−7.90 (A)**	−7.89 (A)	−7.87 (A)	−7.90 (A)	**−7.89 (A)**	−7.85 (A)	−7.84 (A)	−7.84 (A)	−7.83 (A)	−7.82 (A)	−7.80 (A)
MO59, 60	**−7.92 (E)**	−7.97 (E)	−8.02 (E)	−8.08 (E)	**−8.10 (E)**	−8.09 (E)	−8.11 (E)	−8.12 (E)	−8.12 (E)	−8.11 (E)	−8.10 (E)

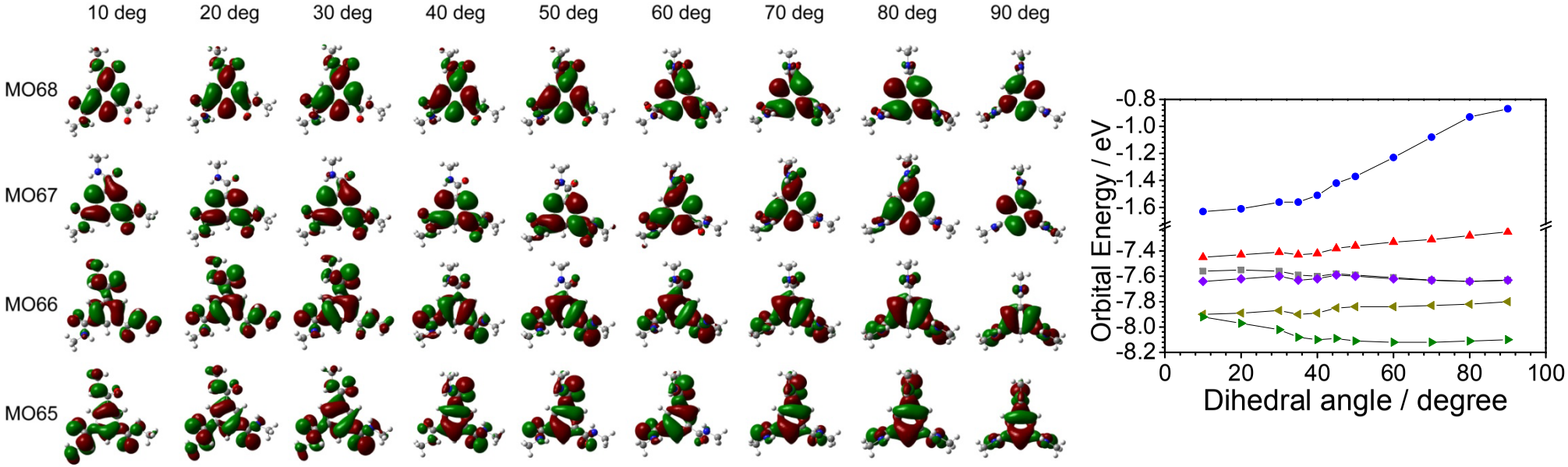

Figure S11 Molecular orbitals in HOMO-LUMO region of BTA **1e** with the C=O dihedral angles between 10° and 90° by 10° interval. The plot of the orbital energy against the dihedral angle is shown in the right graph, blue circle: MO67, 68; red upper triangle: MO65, 66; gray square: MO64 (10°~70°) or MO62 (80° and 90°); purple diamond: MO62, 63 (10°~70°) or MO63, 64 (80° and 90°); olive left triangle: MO61; green right triangle: MO59, 60. The MO67, 68 (LUMO, LUMO+1) and MO59, 60 (HOMO−7, HOMO−6) showed prominent energy changes as a function of the dihedral angle.

Table S9 The extreme wavelength, rotatory strength, and CD epsilon values at the first and second transition with the C=O dihedral angles between 20° and 50° obtained from TD-DFT calculation

C=O dihedral angle	Wavelength [nm]		Rotatory strength [-]			CD epsilon [-]		
	1st transition	2nd transition	1st transition	2nd transition	Ratio (1st/2nd)	1st transition	2nd transition	Ratio (1st/2nd)
20°	266.5	240.8	3.011	14.83	0.20	191.99	734.19	0.26
30°	264.2	237.4	10.86	54.16	0.20	379.50	786.52	0.48
35°	262.8	236.4	15.23	48.27	0.32	486.42	752.28	0.65
40°	260.5	234.9	20.54	41.15	0.50	611.69	697.75	0.88
45°	257.7	232.7	26.02	35.37	0.74	737.90	647.60	1.14
50°	254.7	230.7	31.28	28.04	1.12	860.15	544.08	1.58

Supplementary Material (ESI) for Chemical Science
This journal is © The Royal Society of Chemistry 2011

References

[1] P. J. M. Stals, M. M. J. Smulders, R. Martín-Rapún, A. R. A. Palmans and E. W. Meijer, *Chem. Eur. J.*, 2009, **15**, 2071–2080.

[2] Gaussian 03, Revision D.01, M. J. Frisch, G. W. Trucks, H. B. Schlegel, G. E. Scuseria, M. A. Robb, J. R. Cheeseman, J. A. Montgomery, Jr., T. Vreven, K. N. Kudin, J. C. Burant, J. M. Millam, S. S. Iyengar, J. Tomasi, V. Barone, B. Mennucci, M. Cossi, G. Scalmani, N. Rega, G. A. Petersson, H. Nakatsuji, M. Hada, M. Ehara, K. Toyota, R. Fukuda, J. Hasegawa, M. Ishida, T. Nakajima, Y. Honda, O. Kitao, H. Nakai, M. Klene, X. Li, J. E. Knox, H. P. Hratchian, J. B. Cross, V. Bakken, C. Adamo, J. Jaramillo, R. Gomperts, R. E. Stratmann, O. Yazyev, A. J. Austin, R. Cammi, C. Pomelli, J. W. Ochterski, P. Y. Ayala, K. Morokuma, G. A. Voth, P. Salvador, J. J. Dannenberg, V. G. Zakrzewski, S. Dapprich, A. D. Daniels, M. C. Strain, O. Farkas, D. K. Malick, A. D. Rabuck, K. Raghavachari, J. B. Foresman, J. V. Ortiz, Q. Cui, A. G. Baboul, S. Clifford, J. Cioslowski, B. B. Stefanov, G. Liu, A. Liashenko, P. Piskorz, I. Komaromi, R. L. Martin, D. J. Fox, T. Keith, M. A. Al-Laham, C. Y. Peng, A. Nanayakkara, M. Challacombe, P. M. W. Gill, B. Johnson, W. Chen, M. W. Wong, C. Gonzalez, and J. A. Pople, Gaussian, Inc., Wallingford CT, 2004.

[3] (a) C. Adamo and V. Barone, *J. Chem. Phys.*, 1999, **110**, 6158–6170; (b) D. Jacquemin, J. Preat, V. Wathelet, M. Fontaine and E. A. Perpète, *J. Am. Chem. Soc.*, 2006, **128**, 2072–2083; (c) D. Jacquemin, E. A. Perpète, G. E. Scuseria, I. Ciofine and C. Adamo, *J. Chem. Theory Comput.*, 2008, **4**, 123–135.

[4] N. M. O'Boyle, A. L. Tenderholt and K. M. Langner, *J. Comput. Chem.*, 2008, **29**, 839−845.